This article was downloaded by: [University Of Gujrat]
On: 11 December 2014, At: 13:50
Publisher: Taylor & Francis
Informa Ltd Registered in England and Wales Registered Number: 1072954 Registered office: Mortimer House, 37-41 Mortimer Street, London W1T 3JH, UK

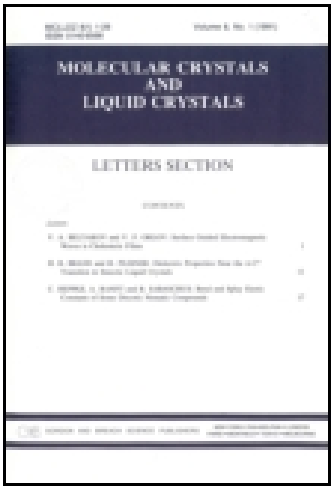

Molecular Crystals and Liquid Crystals
Publication details, including instructions for authors and subscription information:
http://www.tandfonline.com/loi/gmcl20

The Effect of Phosphor-TiO_2 Layer on the Performance of Dye-Sensitized Solar Cells

Seong Gwan Shin[a], Chung Wung Bark[a] & Hyung Wook Choi[a]
[a] Department of Electrical Engineering, Gachon University, Sujeong-Gu, Seongnam-Si, Gyeonggi-Do, Korea
Published online: 17 Nov 2014.

To cite this article: Seong Gwan Shin, Chung Wung Bark & Hyung Wook Choi (2014) The Effect of Phosphor-TiO_2 Layer on the Performance of Dye-Sensitized Solar Cells, Molecular Crystals and Liquid Crystals, 600:1, 47-55, DOI: 10.1080/15421406.2014.936770

To link to this article: http://dx.doi.org/10.1080/15421406.2014.936770

PLEASE SCROLL DOWN FOR ARTICLE

Taylor & Francis makes every effort to ensure the accuracy of all the information (the "Content") contained in the publications on our platform. However, Taylor & Francis, our agents, and our licensors make no representations or warranties whatsoever as to the accuracy, completeness, or suitability for any purpose of the Content. Any opinions and views expressed in this publication are the opinions and views of the authors, and are not the views of or endorsed by Taylor & Francis. The accuracy of the Content should not be relied upon and should be independently verified with primary sources of information. Taylor and Francis shall not be liable for any losses, actions, claims, proceedings, demands, costs, expenses, damages, and other liabilities whatsoever or howsoever caused arising directly or indirectly in connection with, in relation to or arising out of the use of the Content.

This article may be used for research, teaching, and private study purposes. Any substantial or systematic reproduction, redistribution, reselling, loan, sub-licensing, systematic supply, or distribution in any form to anyone is expressly forbidden. Terms & Conditions of access and use can be found at http://www.tandfonline.com/page/terms-and-conditions

Mol. Cryst. Liq. Cryst., Vol. 600: pp. 47–55, 2014
Copyright © Taylor & Francis Group, LLC
ISSN: 1542-1406 print/1563-5287 online
DOI: 10.1080/15421406.2014.936770

Taylor & Francis
Taylor & Francis Group

The Effect of Phosphor-TiO_2 Layer on the Performance of Dye-Sensitized Solar Cells

SEONG GWAN SHIN, CHUNG WUNG BARK, AND HYUNG WOOK CHOI*

Department of Electrical Engineering, Gachon University, Sujeong-Gu, Seongnam-Si, Gyeonggi-Do, Korea

Downloaded by [University Of Gujrat] at 13:50 11 December 2014

Dye-sensitized solar cells (DSSCs) are composed of an electrode made of a dye-adsorbed nanoporous TiO_2 layer on a fluorine-doped tin oxide (FTO) glass substrate, redox electrolytes, and a counter electrode. In this study, phosphor is introduced into the TiO_2-layer electrode of a DSSC. The admixed phosphor content in the TiO_2 paste is varied from 1.0 to 10.0 wt%. By a conversion-luminescence process, $ZnGa_2O_4:Mn^{2+}$ phosphor improves light harvesting and increases the photocurrent. The phosphor elevates both, the energy level of electrons in the oxide film and V_{oc} of the DSSC. Using a TiO_2 electrode containing 5.00 wt% of admixed $ZnGa_2O_4:Mn^{2+}$, the light-to-electricity energy-conversion efficiency of the DSSC reaches 8.02%, which is higher by a factor of 1.25 than that of a DSSC without $ZnGa_2O_4:Mn^{2+}$.

Keywords TiO_2; phosphor; DSSCs; nanoparticles

Introduction

Dye-sensitized solar cells (DSSCs) have been intensively studied since their discovery in 1991 [1–7]. DSSCs have been attracting considerable attention around the world because of their reasonable conversion efficiency, low production cost, and simple fabrication process, compared to silicon solar cells [8–16]. A DSSC is composed of an electrode made of a dye-adsorbed nanoporous TiO_2 layer on a fluorine-doped tin oxide (FTO) glass substrate, redox electrolytes, and a counter electrode. One of the ways to increase the efficiency of DSSCs is to enhance the harvesting of light [17–19]. Many synthetic dyes have been synthesized and employed to improve the harvest of light and to increase the photocurrent production of DSSCs; however, even the best dyes (N-719) only absorb in the wavelength range of 400–800 nm, [20–21], and most of the ultraviolet region is not used. If ultraviolet radiation could be converted to visible light by a suitable conversion-luminescence process and reabsorbed by the dye of a DSSC, a larger part of the solar irradiation could be used and the photocurrent of the DSSC will be effectively enhanced. Furthermore, the open-circuit voltage (V_{oc}) of the DSSC depends on the energy level of the electrons in the oxide film

*Address correspondence to Prof. Hyung Wook Choi, Department of Electrical Engineering, Gachon University, 1342 SeongnamDaero, Sujeong-Gu, Seongnam-Si, Gyeonggi-Do 461-701, Korea (ROK). Tel.: (+82)31-750-5562; Fax: (+82)31-750-8833. E-mail: chw@Gachon.ac.kr

Color versions of one or more of the figures in the article can be found online at www.tandfonline.com/gmcl.

[20, 22]. If the electronic energy level could be heightened by a phosphor layer, V_{oc} of a DSSC will be increased.

In this work, $ZnGa_2O_4:Mn^{2+}$ phosphor is introduced to the TiO_2 photoelectrode of a DSSC to improve light harvesting, photovoltage, photocurrent production, and solar conversion efficiency by a conversion-luminescence process. Combining excitation and emission spectra, the ultraviolet region of the solar irradiation can be reabsorbed by dye N-719 after conversion luminescence by $ZnGa_2O_4:Mn^{2+}$ and, consequently, the solar light harvest of the DSSCs could be increased. Moreover, by introduction of the phosphor layer, it is possible to further increase the conversion efficiency of the DSSC.

Experimental

Preparation of $ZnGa_2O_4:Mn^{2+}$ Powder

The nanocrystalline $ZnGa_2O_4:Mn^{2+}$ phosphors were prepared by the precipitation method.[23] $ZnSO_4 \cdot 7H_2O$ (99.99%, Aldrich), $Ga_2(SO_4)_3 \cdot 6H_2O$ (99.99%, Aldrich), and $MnSO_4 \cdot xH_2O$ (99.99%, Aldrich) were used as starting materials and aqueous NH_4OH (NH_3 content 28–30%, Sigma Aldrich) was used as precipitant. The starting solutions were prepared by dissolving equimolar amounts of manganese sulfate, zinc sulfate and gallium sulfate in distilled water. (with a final concentration of 0.1 mol/dm^3) Aqueous ammonia solution with a concentration of 0.89 mol/dm^3 was prepared and used in the experiments.

The starting metal solution was added to the aqueous ammonia solution at 90°C upon stirring, done at a rate of 1.5 ml/min for 20 h. The metal ions were rapidly hydrolyzed by ammonia and precipitation occurred spontaneously. The precipitation experiment was performed using a reflux system to preserve the concentrations over the entire experimental period. The precipitates were separated by filtration through a membrane filter, washed with distilled water, and then dried for 4 h in an oven at 60°C. The nanocrystalline $ZnGa_2O_4:Mn^{2+}$ powders thus obtained were sieved to deagglomerate the particles, and then sintered at 1000°C for 1 h using alumina crucibles in a furnace.

Preparation of the Film Electrodes of the DSSCs

Titanium(IV) isopropoxide (TTIP, Sigma Aldrich), ethyl alcohol, nitric acid, and de-ionized (DI) water were used as the precursors. As-prepared TiO_2 particles were calcined in air at 450°C for 1 h, using a programmable furnace, to obtain the desired stoichiometry and crystallinity. The phosphor(1-10.00 wt.%)-mixed TiO_2 pastes were prepared as per the Figure 1. A TiO_2 paste was prepared by coating an FTO plate using a doctor blade technique, then, the $ZnGa_2O_4:Mn^{2+}$-TiO_2 layer was coated on top of the TiO_2 film by the same method. The electrodes (TiO_2-$ZnGa_2O_4:Mn^{2+}$) were sintered at 500°C for 15 min in air and, subsequently, immersed in dye N-719 for 24 h at room temperature. For comparison, a dye-sensitized TiO_2 electrode without $ZnGa_2O_4:Mn^{2+}$ was prepared. A counter electrode was prepared by spin coating an H_2PtCl_6 solution onto an FTO glass and heating to 450°C for 30 min. The dye-adsorbed TiO_2 electrode and the Pt counter electrode were assembled to a sandwich-type cell and sealed with a 60-μm thick hot-melt sealant. An electrolytic solution was introduced through a hole drilled in the counter electrode. The hole was then sealed using a cover glass.

Downloaded by [University Of Gujrat] at 13:50 11 December 2014

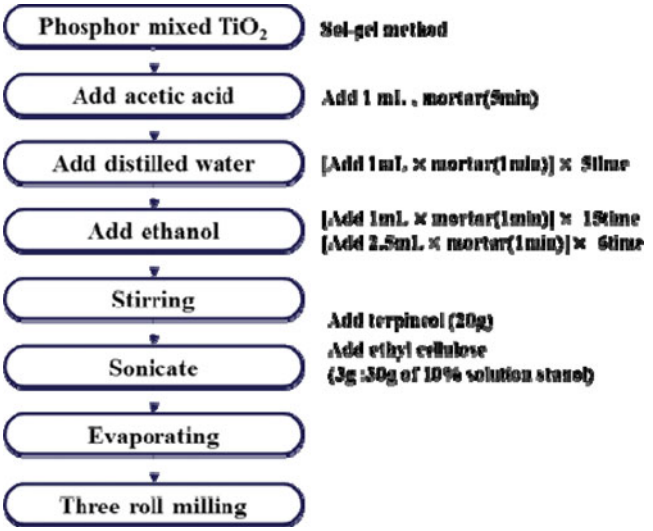

Figure 1. Flowchart for the preparation of the phosphor mixed TiO_2.

Measurements

The phase identification of the fabricated photoelectrode was performed by X-ray diffraction (XRD) using a Rigaku D/MAX-2200 diffractometer with Cu Kα radiation. Photoluminescence (PL) spectra were recorded using a 150 W Xe lamp (spectrofluorometer, FP-6200, JASCO). The morphology of the prepared phosphor-admixed TiO_2 layer was investigated by field-emission scanning electron microscopy (FE-SEM, model S-4700, Hitachi). The absorption spectra of the TiO_2-electrode films were measured using a UV-vis spectrometer (UV-vis 8453, Agilent). The conversion efficiency of the fabricated DSSCs was measured using an I–V solar simulator (Solar Simulator, McScience). The active area of the resulting cell exposed to light was approximately 0.25 cm^2 (0.5 cm $\times$ 0.5 cm).

Results and Discussion

Figure 2(a) shows the XRD pattern of the $ZnGa_2O_4$:Mn^{2+} phosphor. The XRD pattern shows various peaks including the (311) peak. The XRD patterns of all investigated samples were in good agreement with JCPDS card no. 38-1240, indicating that $ZnGa_2O_4$ forms the expected spinel structure at a sintering temperature of 1000°C. No second phase can be detected, indicating that the Mn^{2+} ions can be effectively built into the $ZnGa_2O_4$ host lattice by substitution for the Zn^{2+} ions. Figure 2(b) shows the XRD pattern of TiO_2 nanoparticles after sintering at 500°C, which indicates a mixture of the anatase and rutile phases. The XRD pattern of TiO_2 nanoparticles shows prominent (101), (004), and (200) anatase peaks, as well as pronounced (110) and (101) rutile peaks. The XRD pattern shown in Figure 2(c) was observed in case of the phosphor-admixed TiO2 surface, revealing crystallinity at the most prominent peaks originating from the phosphor being indicated by P1-P4.

Figure 3 shows a SEM image of the $ZnGa_2O_4$:Mn^{2+} phosphor. It can be seen that the particle size is about 50 nm after sintering at a temperature of 1000°C. It can be seen that the phosphor prepared by the precipitation method shows relatively uniform, dispersive,

Downloaded by [University Of Gujrat] at 13:50 11 December 2014

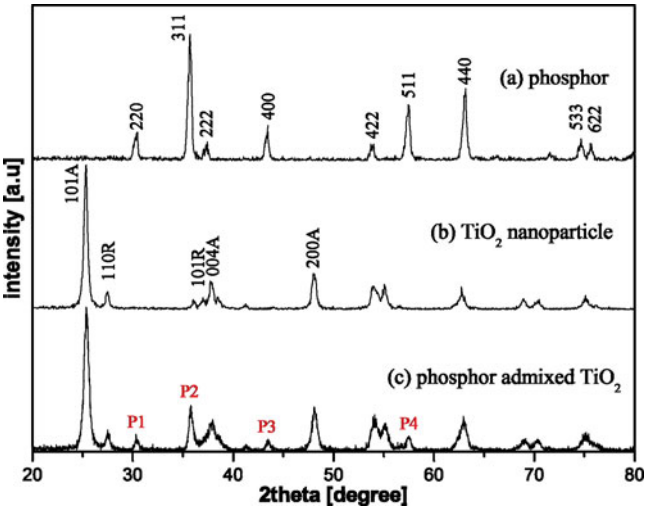

Figure 2. XRD patterns of (a) phosphor, (b) TiO_2 nanoparticles, and (c) phosphor-admixed TiO_2.

and nearly spherical morphology. It is well known that the luminescent properties of a phosphor powder are dependent upon its particle size and size distribution. Finer particles tend to have more surface luminous states arising from their increased surface/bulk volume ratio. This may result in nano size crystals are favorable for photoluminescence [24–25]. Phosphor particles with a uniform size are thus beneficial to highly efficient and uniform luminescence [26].

The excitation and emission spectra of phosphor-admixed TiO_2 are given in Figure 4(a) and (b), respectively. It can be seen from Figure 4(a) that a broad excitation band appears at a peak wavelength of 304 nm. The strong excitation band with a maximum at 304 nm is due to a change-transfer transition of Mn^{2+}, one of the d–d transitions within the Mn^{2+} $3d^5$ configuration [27]. This excitation absorption band implies that ultraviolet

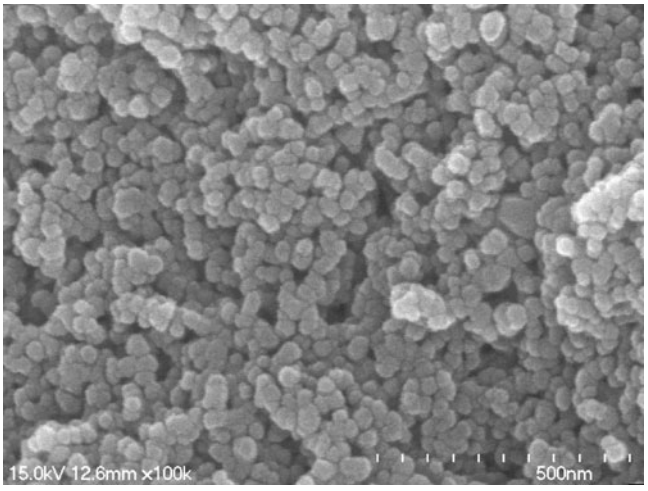

Figure 3. SEM image of the $ZnGa_2O_4$:Mn^{2+} phosphor.

Downloaded by [University Of Gujrat] at 13:50 11 December 2014

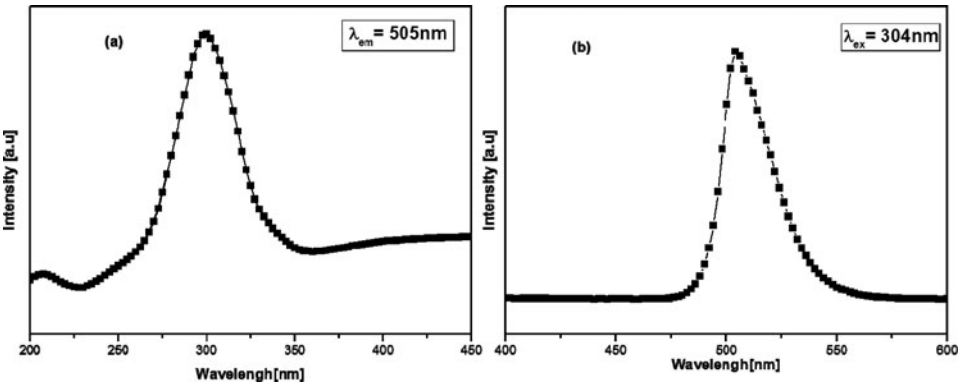

Figure 4. (a) PL excitation spectrum and (b) PL emission spectrum of phosphor-admixed TiO_2.

Downloaded by [University Of Gujrat] at 13:50 11 December 2014

irradiation from the sun can be absorbed by $ZnGa_2O_4:Mn^{2+}$. Figure 4(b) shows the emission spectra of phosphor-admixed TiO_2. It can be seen that $ZnGa_2O_4:Mn^{2+}$ exhibits an obvious luminescence function. The emission spectrum with its maximum around 505 nm, excited by 304 nm, is attributed to the transition $^4T_1$-$^6A_1$ of the 3d electrons of the Mn^{2+} ion [28–29] which occupies the tetrahedrally coordinated Zn position of the host material [30]. The luminescence around 505 nm is just within the absorption wavelength range of the sensitizing dye N-719 [20–21]. Combining excitation and emission spectra, the ultraviolet region of the solar radiation can be reabsorbed by the dye N-719 via conversion luminescence by $ZnGa_2O_4:Mn^{2+}$ and, therefore, the solar light harvest of corresponding DSSCs may be increased.

Figure 5 shows the UV-vis absorbance of phosphor-admixed TiO_2 for different phosphor content. The absorption spectrum of $ZnGa_2O_4:Mn^{2+}$ phosphor has a peak at ultraviolet ray area [31]. And N-719 only absorb visible light in the wavelength range 400–800 nm

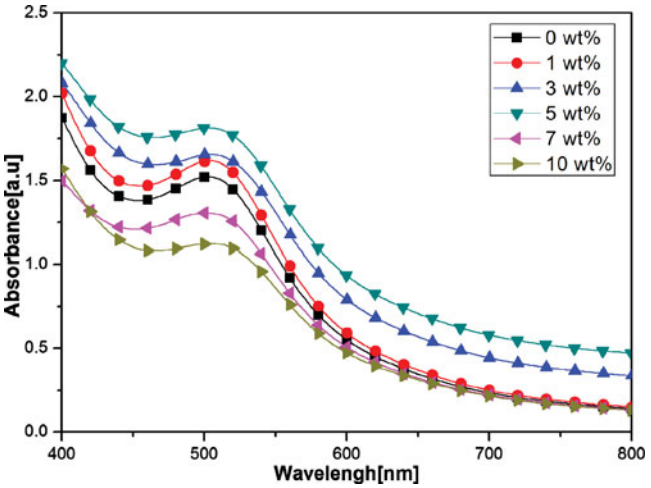

Figure 5. UV-vis absorbance of phosphor-admixed TiO_2 for different phosphor concentrations.

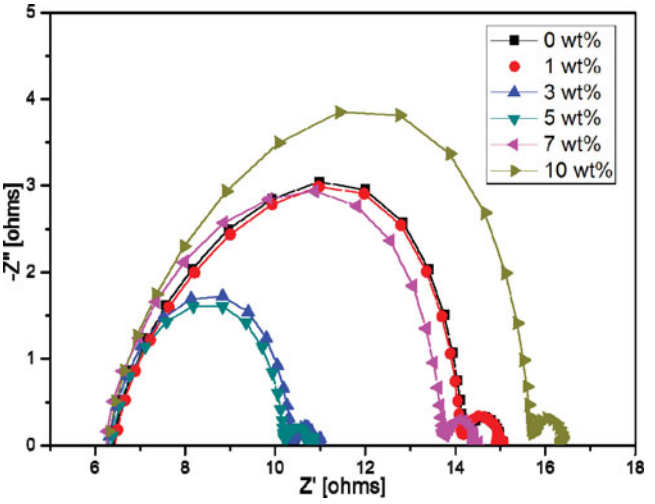

Figure 6. EIS Nyquist plots of DSSCs with phosphor-admixed TiO_2 electrode for different phosphor concentrations.

[20]. It can be seen in Figure 5 that in the entire wavelength range of 400–800 nm, the absorbance spectra for the sample with a phosphor content of 5.00 wt% was highest. Figure 5 shows that in the wavelength range of 400–800 nm, the absorbance spectra of DSSCs with a phosphor-admixed TiO_2 layer are higher than without phosphor. Obviously, this is due to the conversion luminescence of the phosphor and the resulting reabsorption by the dye of the DSSCs.

Figure 6 shows electrochemical impedance spectroscopy (EIS) Nyquist plots of DSSCs with phosphor-admixed TiO_2 electrode. EIS is a useful method for the analysis of charge-transport processes and internal resistances [32]. As shown in Figure 6, there is a decrease in the charge-transfer resistance (R_{ct}) upon increasing phosphor amount varying from 0%

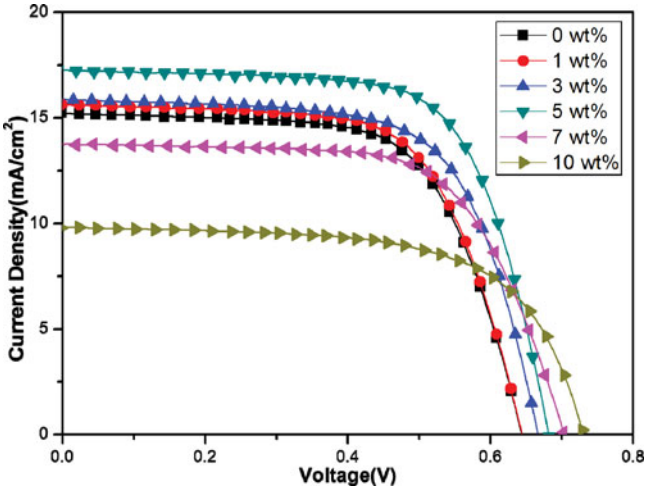

Figure 7. I–V characteristic of DSSCs.

Downloaded by [University Of Gujrat] at 13:50 11 December 2014

Table 1. J_{sc}, V_{oc}, FF, and efficiency

Phosphor content	J_{sc} (mA/cm^2)	V_{oc} (V)	FF (%)	Efficiency (η)
0 wt%	15.25	0.6437	65.36	6.41
1 wt%	15.64	0.6441	65.50	6.59
3 wt%	15.89	0.6663	66.22	7.01
5 wt%	17.26	0.6810	68.46	8.04
7 wt%	13.77	0.7028	65.88	6.37
10 wt%	9.8	0.7300	64.29	4.60

Downloaded by [University Of Gujrat] at 13:50 11 December 2014

to 5%. This increases the number of injected electrons into the TiO_2 layer, improves the electrical conductivity, and reduces the charge recombination at the TiO_2/dye/electrolyte interface [33–34]. R_{ct} directly affects the fill factor (FF) of a DSSC. If R_{ct} decreases, FF increases and, consequently, the efficiency of the cell also increases [35]. However, R_{ct} becomes larger when the phosphor content is more than 10%. The enlargement of R_{ct} means an increase of the recombination rate and indicates slow electron-transfer processes in the DSSCs. The reason is that with the increase of the $ZnGa_2O_4$:Mn^{2+} content in TiO_2, crystal defects are produced that cause a higher electron transport resistance [36]. The inefficient charge-transfer paths increase the recombination rate of electrons with I^{3-} or the oxidizing dye, resulting in a low photocurrent density and conversion efficiency [37].

Figure 7 shows the current–voltage photovoltaic performance curves of DSSCs with pure and phosphor-admixed TiO_2 under AM 1.5 illumination (100 mW/cm^2). Table 1 summarizes the efficiency, FF, open-circuit voltage, and short-circuit current of the corresponding solar cells. J_{sc} changes significantly because of the effect of the admixed phosphor. As shown in Table 1, J_{sc} increases with the amount of phosphor increase until the phosphor content is 5.00 wt%, beyond of which J_{sc} decreases. The increase in J_{sc} is mainly due to the conversion luminescence of phosphor, which facilitates the harvest of more incident light [38]. The decrease in Jsc is due to the fact that introduction of phosphor produces defects in the oxide film, which causes the recombination of photoinduced holes and electrons and the decrease of Jsc [36]. Furthermore, V_{oc} increases on increasing percentage of $ZnGa_2O_4$:Mn^{2+}. V_{oc} of the DSSCs depends on the energy level of the electrons in the oxide film and the redox potential of the electrolyte [20,22]. If Mn^{2+} ions substitute Ti^{4+} ions at the Ti-lattice sites in TiO_2, the electronic energy level of the oxide film is elevated, which leads to an increase of V_{oc}.[39–40] If a phosphor-admixed (5.0 wt%) TiO_2 electrode is used in DSSCs, a light-to-electric energy conversion efficiency of 8.04%, a short-circuit current density of 17.26 mA/cm^2, an open-circuit voltage of 0.6810 V, and an FF of 68.46% is achieved. Higher efficiencies were achieved for DSSCs with phosphor-admixed TiO_2 than for cells with pure TiO_2 nanoparticles.

Conclusions

The photovoltaic performances of DSSCs with phosphor-admixed TiO_2 (1.0–10.00 wt%) were compared. The conversion luminescence of phosphor improves both, the light harvest and J_{sc}. As R_{ct} decreases, FF increases and, consequently, also the efficiency of the cell. The addition of phosphor elevates both the energy level of the oxide film and V_{oc} of the DSSC. In case of a TiO_2 electrode with 5.00 wt% of $ZnGa_2O_4$:Mn^{2+}, the light-to-electric energy conversion efficiency of the DSSC reaches 8.04% under a simulated solar light irradiation

of 100 mW/cm^2, which is higher by a factor of 1.25 than the efficiency of DSSCs without phosphor. DSSCs based on phosphor-admixed TiO_2 show better photovoltaic performances than cells with pure TiO_2 nanoparticles.

Funding

This work was supported by the Human Resources Development program (No. 20124030200010) of the Korea Institute of Energy Technology Evaluation and Planning (KETEP) grant funded by the Korea government Ministry of Trade, Industry and Energy. This work was also supported by the National Research Foundation of Korea (NRF) Grant funded by the Korean Government (MEST) (No. 2012R1A1A2044472).

References

[1] Gratzel, M. (2004). *J.Photochem. Photobiol. A.*, *164*, 3.
[2] O'Regan, B., & Gratzel, M. (2004). *Nature.*, *353*, 737.
[3] Chappel, S., Chen, S. G., & Zaban, A. (2002). *Langmuir*, *18*, p.3336.
[4] Bedja, I., Kamat, P. V., Hua, X., Lappin, A. G., & Hotchandani, S. (1997). *Langmuir*, *13*, p.2398.
[5] Keis, K., Bauer, C., Boschloo, G., Hagfeldt, A., Westermark, K., Rensmo, H., & Siegbahn, H. (2002). *J. Photochem. Photobiol. Chem.*, *148*, p.57.
[6] Chappel, S., & Zaban, A. (2002). *Solar Energy Mater Solar Cells*, *71*, p.141.
[7] Guo, P., & Aegerter, M. A. (1999). *Thin Solid Films*, *351*, p.290.
[8] Xia, J., Masaki, N., Jiang, K., Wada, Y., & Yanagida, S. (2006). *Chem. Lett.*, *35*, 252.
[9] Gratzel, M. (2005). *Inorg. Chem.*, *44*, 6841.
[10] Hamann, T. W., Jensen, R. A., Martinson, A. B. F., Ryswyk, H. V., & Hupp, J. T. (2008). *Energ. Environ. Sci.*, *1*, 66.
[11] Kong, F. T., Dai, S.-Y., & Wang, K. J. (2007). *Adv. Opto. Elect*, 75384.
[12] Prakash, T. (2012). *Electronic materials Letters*, Vol. *8*, No. 3, pp.231–243.
[13] Huh, P., & Kim, S. C. (2012). *Electronic materials Letters*, Vol. *8*, pp.131–134.
[14] Hara, K., Tachibana, Y., Ohga, Y., Shinpo, A., Suga, S., Sayama, K., Sugihara, H., & Arakawa, H. (2003). *Solar Energy materials and Solar cells*, *77*, 89.
[15] Matsui, H., Okada, K., Kawashima, T., *et al.*, (2004). *A: Chemistry*, *164*, 129.
[16] Kim, S. S., Nah, Y. C., Noh, Y. Y., Jo, J., & Kim, D. Y. (2006). *Electrochimica Acta*, *51*, 3814.
[17] Oelhafen, P., & Schuler, A. (2005). *Solar Energy*, *79*, 110–121.
[18] Yang, Guangtao, Zhang, Jing, Wang, Peiqing, Sun, Qiang, Zheng, Jun, & Zhu, Yuejin (2011). *Current Applied Physics*, Vol.*11*, pp. 376–381.
[19] Wang, Yuanzhe, Chen, Enlong, Lai, Hongmei, Lu, Bin, Hu, Zhijuan, Qin, Xiaomei, Shi, Wangzhou, & Du, Guoping (2013). *Ceramics International*, Vol. *39*, pp. 5407–5413.
[20] Gratzel, M. (2001). *Nature*, *414*, pp.338.
[21] Shen, Heping, Li, Xin, Li, Jianbao, Wang, Wenli, Lin, Hong (2013). *Electrochimica Acta*, Vol.*97*, pp.160–166.
[22] Gratzel, M., & Gratzel, M. (2009). *Acc. Chem. Res.*, *42*, p.1788.
[23] Cha, J. H., Kim, K. H., Park, Y. S., Park, S. J., & Choi, H.W., (2009). *Mol. Cryst. Liq. Cryst.*, Vol. *499*, pp. 85.
[24] Yu, I. (2006). *Mater. Res. Bull.*, *41*, pp. 1403–1406.
[25] Shin, S. H., kang, J. H., Jeon, D. Y., & Zang, D. S. (2005) *J. Solid State Chem.*, *178*, pp. 2205–2210.
[26] Li, J. G., Li, X. D., Sun, X. D., & Ishigaki, T. (2008). *J. Phys. Chem. C*, *112*, pp. 11707–11716.
[27] Yu, M., Lin, J., Zhou, Y. H., & Wang, S. B. (2002) *erials Letters*, *56*, pp.1007–1013.
[28] Cha, J. H., Kim, K. H., Park, Y. S., Kwon, S. J., & Choi, H. W. (2007). *Jpn. J. Appl. Phys.*, Vol. *46*, pp. 6702–6704.

Downloaded by [University Of Gujrat] at 13:50 11 December 2014

[29] ParkJ. H., Lee, S. H., Kim, J. S., Park, H. W., Choi, J. C., Park, H. L., Kim, G. C., & Yoo, J. H. (2007). *journal of Crystal Growth*, *299*, 369–373.
[30] Kim, J. S., Kim, J. S., Kim, T. W., Kim, S. M., & Park, H. L. (2005). *Appl. Phys. Lett.*, *86*, pp.091912.
[31] Masahiro, T., Morio, O., & Tetsuhiko, I. (2009) *Journal of Physics and Chemistry of Solids*, Vol. *70*, pp.281–285.
[32] Yang C. C., Zhang, H. Q., & Zheng, Y. R. (2011). *Supplement, January*, Volume *11*, pp. S147–S153.
[33] Fabregat-Santiago, F., Bisquert, J., Palomares, E., Otero, L., Kuang, D., Zakeeruddin, S. M., & Grätzel, M. (2007). *J. Phys. Chem. C*, *111*, pp.6550–6560.
[34] Kern, R., Sastrawan, R., Ferber, J., Stangl, R., & Luther, J. (2002). *Electrochim. Acta*, *47*, pp.4213–4225.
[35] Gagliardi, S., Giorgi, L., Giorgi, R., Lisi, N., Dikonimos Makris, Th., Salernitano, E., & Rufoloni, A. (2009). *Superlattices and Microstructures*, *46*, pp.205–208.
[36] Murakoshi, K., Kano, G., Wada, Y., Yanagida, S., Miyazaki, H., Matsumoto, M., & Murasawa, S. (1995). *J. Electroanal. Chem.*, *396*, p.27.
[37] Zhong, Min, Shi, Jingying, Zhang, Wenhua, Han, Hongxian, & Li, Can (2011). *Materials Science and Engineering B*, *176*, pp.1115–1122.
[38] Chou, C. S., Guo, M. G., Liu, K. H., & Chen, Y. S. (2012). *Applied Energy*, Volume *92*, pp.224–233.
[39] Ko, K., Lee, Y., & Jung, Y. (2005). *J. Colloid Interface Sci.*, *283*, pp. 482.
[40] Liau, L., & Lin, C. (2008). *Thin Solid Films*, *516*, pp. 1998.

Downloaded by [University Of Gujrat] at 13:50 11 December 2014